Definition of parametric methods for fault analysis applied to an electromechanical servomechanism affected by multiple failures

Paolo Maggiore[1], Matteo D. L. Dalla Vedova[2], Lorenzo Pace[3] and Alessio Desando[4]

[1,2,3,4]*Politecnico di Torino, Torino, 10129, Italy*

paolo.maggiore@polito.it
matteo.dallavedova@polito.it
lorenzo.pace@polito.it
alessio.desando@polito.it

ABSTRACT

In order to detect incipient failures due to a progressive wear of a primary flight command electromechanical actuator, prognostics could employ several approaches; the choice of the best ones is driven by the efficacy shown in failure detection, since not all the algorithms might be useful for the proposed purpose. In other words, some of them could be suitable only for certain applications while they could not give useful results for others.

Developing a fault detection algorithm able to identify the precursors of the above mentioned electromechanical actuator (EMA) failure and its degradation pattern is thus beneficial for anticipating the incoming failure and alerting the maintenance crew such to properly schedule the servomechanism replacement.

The research presented in the paper was focused to develop a prognostic technique, able to identify symptoms alerting that an EMA component is degrading and will eventually exhibit an anomalous behavior; in particular four kinds of failure are considered: friction, backlash, coil short circuit, rotor static eccentricity. To this purpose, an innovative model based fault detection technique has been developed merging together several information achieved by means of FFT analysis and proper "failure precursors" (calculated by comparing the actual EMA responses with the expected ones). To assess the robustness of the proposed technique, an appropriate simulation test environment was developed.

The results showed an adequate robustness and confidence was gained in the ability to early identify an eventual EMA malfunctioning with low risk of false alarms or missed failures.

1. INTRODUCTION

Prognostics is a discipline whose purpose is to predict the moment in which a certain component loses its functionality and is not further able to meet desired performances. It is based on analysis and knowledge of its possible failure modalities and on the capability to individuate the first signs of aging or wear and, then, evaluate the magnitude of such damage (fault detection / evaluation). The above mentioned data will be then used as input of a proper failure propagation model.

The use of this discipline in aeronautics, as in many other technological fields, could be very useful if applied to maintenance, since it lowers both costs and inspection time. In order to optimize these advantages, the discipline known as Prognostics and Health Management (PHM) has born: its purpose is to provide real-time data on the current status of the system and to calculate the Remaining Useful Life (RUL) before a fault occurs or a component becomes unable to perform its functionalities at a desired level. The advantages gained by means of PHM strategies are evident comparing the features of a system conceived according to this discipline with the ones of a classical design.

The primary flight controls are a critical feature of the aircraft system and are therefore designed with a conservative safe-life approach which imposes to replace the related components subsequently to a certain number of flight hours (or operating cycles): obviously, this approach is not able to evaluate the effective status of the items (and estimate the ability to operate still correctly) but merely requires the aforesaid maintenance operations.

In particular, the aforesaid design criterion is not able to evaluate possible initial flaws (occurred during manufacturing) that could generate a sudden fault which could compromise the safety of the aircraft and don't allow to replace only the really failed components (with the related inefficiencies and additional costs).

Instead, in a system suitably conceived taking into account the PHM strategies, failures could be managed in a more proper way, obtaining the following advantages:

1. lower operating costs;
2. less maintenance interventions are required;
3. lower number of redundancies installed on board aircraft;
4. aircraft safety and reliability are improved;
5. any maintenance work can be planned appropriately optimizing the necessary actions (limiting downtime and related costs and allowing a more effective organization of the maintenance and management of spare parts warehouses) and limiting the logistical difficulties resulting from the manifestation of the fault.

The research presented in the paper was focused to develop a fault detection/evaluation technique able to identify failure precursors (alerting that the system is degrading) and to evaluate the corresponding damage entity; in fact, a progressive degradation of a system component, which does not initially create an unacceptable behavior, often leads to a condition in which the efficiency of such component is impaired and hence the whole actuation system operation could be compromised. In order to develop the above mentioned research, a typical aircraft primary command EMA has been modeled in the MATLAB Simulink® simulation environment and several sets of simulations (in nominal conditions or with various failures) have been performed.

2. AIM OF WORK

The aims of this work are:

1. the proposal of a numerical algorithm able to perform the simulations of the dynamic behavior of a typical electromechanical servomechanism taking into account the effects due to four different types of progressive failures (dry friction, backlash, coil short circuit and rotor static eccentricity);
2. the proposal of an innovative fault detection/evaluation method able to detect the EMA failure precursors and evaluate the corresponding failures entity.

To assess the robustness of the proposed techniques, an appropriate simulation test environment was developed; in particular, in order to evaluate the effects due to the abovementioned failures on the EMA behavior, several simulations (related to different combinations of damages) have been performed. The results obtained from each simulation have been compared with the ones provided by a monitoring model in order to evaluate the related differences and, consequently, define a correlation with the corresponding failures. By means of proper algorithms, the above mentioned results are used to timely identify the failures and evaluate their magnitudes.

To this purpose, an innovative model based prognostic technique has been developed merging together several information achieved by means of FFT analysis and proper "failure precursors" (calculated by comparing the actual EMA responses with the expected ones). The so obtained results showed an adequate robustness and confidence was gained in the ability to early identify the malfunctioning with low risk of false alarms or missed failures.

PROPOSED ACTUATION SYSTEM NUMERICAL MODEL

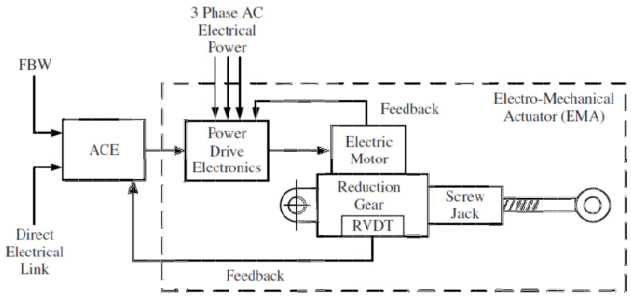

Figure 1. EMA scheme.

As shown in figure 1, a typical electromechanical actuator used in a primary flight control system is composed by:

1. an actuator control electronics (ACE) that closes the feedback loop comparing the commanded position (FBW) with the actual one, elaborates the corrective actions and generates the reference current (*I_ref*);
2. a Power Drive Electronics (PDE) that regulates the three-phase electrical power;
3. an electrical motor, often BLDC type;
4. a gear reducer having the function to decrease the motor (angular) velocity (called RPM) and increase its torque at values suitable for the user[1];
5. a system that transforms rotary motion into linear motion: ball screws or roller screws are usually preferred to acme screws since they, having a higher efficiency, perform the conversion with lower friction;
6. a network of sensors used to close the feedback rings (current, angular speed and position) that control the whole actuation system (reported in Fig. 1 as RVDT).

As previously established, the primary goal of the research is the proposal of a technique able to identify symptoms alerting that an EMA is degrading: therefore, in order to assess the robustness of the aforesaid technique, a suitable simulation test environment has been developed. The proposed numerical model, reported in figure 2, is consistent with the EMA architecture shown in figure 1 and has been implemented in the MATLAB/Simulink® environment.

1 The RPM or torque variations are obviously related to the gear ratio of the mechanical reducer. The output torque (downstream the reducer) is also affected by efficiency of the mechanical transmission.

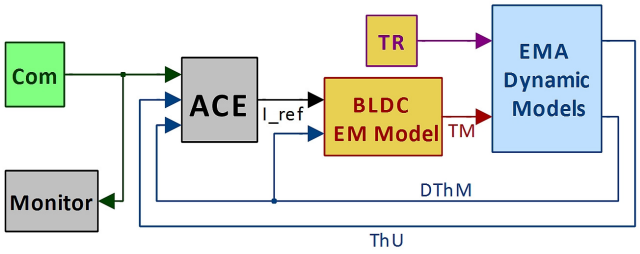

Figure 2. Proposed EMA block diagram developed in MATLAB/Simulink® environment.

It is composed by six different subsystems:

1. an input block that generates the different position commands (Com);
2. a subsystem simulating the actuator control electronics, that close the feedback loops and generates as output the reference current *I_ref* (ACE);
3. a subsystem simulating the power drive electronics and the trapezoidal BLDC electromagnetic model, that evaluates the torque developed by the electrical motor as a function of the voltages generated by the three-phase electrical power regulator (BLDC EM Model);
4. a subsystem simulating the EMA mechanical behavior by means of a 2 degrees of freedom dynamical system (EMA Dynamic Model);
5. another input block simulating the aerodynamic torques acting on the moving surface controlled by the actuator (external forcing TR);
6. a block simulating the EMA monitoring system (Monitor).

The proposed numerical model is also able to simulate the effects due to conversion from analogic to digital of the feedback signals (ADC), electrical noise acting on the signal lines and position transducers affected by electrical offset.

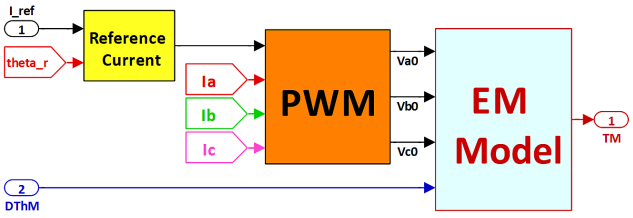

Figure 3. BLDC EM Model block diagram.

Figure 3 shows the numerical simulation algorithm that implements the brushless DC motor electromagnetic model: it is composed by three blocks representing the reference current generator, the three-phase PWM inverter system and the BLDC motor electromagnetic model.

The BLDC EM Model block diagram has been developed according to the mathematical models and the assumption proposed by Çunkas and Aydoğdu (2010) and Halvaei Niasar, Moghbelli and Vahedi (2009).

The trapezoidal back-EMF and the electrical current waveforms of the three-phase BLDC motor, evolving as a function of rotor position (*theta_r*), are shown in figure 4.

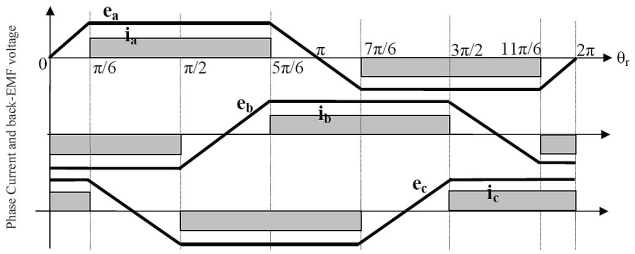

Figure 4. Phase back-EMF and current waveforms of a three-phase BLDC motor.

The motor driving is performed by means of the PWM current control block (figure 5) that compares the reference phase currents (*I_ref_a, I_ref_b, I_ref_c*) with the motor's actual phase currents (*Ia, Ib, Ic*); indeed, the considered block diagram does not implement the structure and the real operation of the three-phase PWM inverter: its behavior is simulated by means of a relay block, having proper thresholds (that user might select), for each phase.

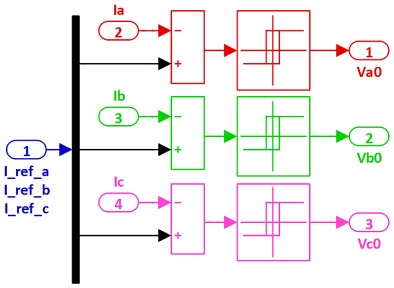

Figure 5. PWM block diagram.

The output of this subsystem, as shown in figure 6, is a three components rotating voltage vector representing the corresponding phase voltages *Va0*, *Vb0* and *Vc0*.

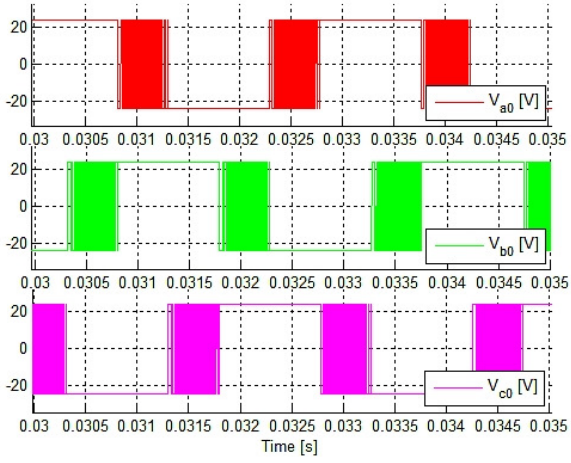

Figure 6. Example of dynamic evolution of the three-phase voltages regulated by PWM block.

As happens for the *I_ref* calculation, at a same instant a phase has a positive value, another has a negative value having the same modulus of the positive one and the remaining one must be null (the proposed model realizes this last statement only on a mean value). The three components show the typical 120 degrees displacement. The EM model (shown in figure 7) calculates the three-phase currents (*Ia, Ib, Ic*) and the developed mechanical torque *TM* as a function of the PWM three phase voltages (*Va0*, *Vb0*, *Vc0*) and the effective rotor velocity *DThM*. The considered BLDC motor has a three-phase winding topology with star connection: it has three resistive (*R*) – inductive (*L*) branches on which a counter-electromotive force[2] (back-EMF) acts. As reported in [2], the back-EMF phase voltages are implemented by using Simulink look-up table functions. It must be noted that the three back-EMF constants *ke_i* (one for each of the three branches) may also take into account some possible electrical failures (like partial coil short circuit or rotor static eccentricity) by modifying the parameters of the functions f(u) (figure 9): these values, multiplied by the effective rotor velocity *DThM*, provide the corresponding real back-EMF values.

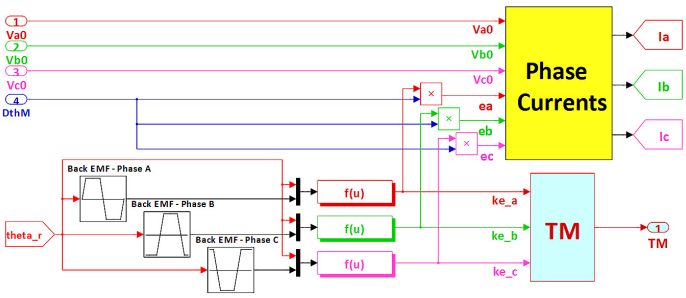

Figure 7. EM Model block diagram.

Since phase currents are known, total motor torque can be computed; this calculation is carried out by the subsystem TM (shown in figure 7): the sum of the three phase currents, multiplied by their respective back-EMF constants *ke* and by the number of polar couples, gives the corresponding value of the total motor torque *TM*.[3]
It must be noted that, in order to validate the just illustrated numerical model, the dynamic response developed by the aforesaid system under certain operating conditions (control input, boundary conditions and entities of different faiths) was compared with data obtained from the literature.

In particular, the back-EMF and phase current waveforms, related to different values of the rotor angular velocity, and the dynamic responses of the BLDC caused by various command inputs have been compared with corresponding cases reported in literature by Lee and Ehsani (2003), highlighting a satisfactory compliance between simulations and literature data.

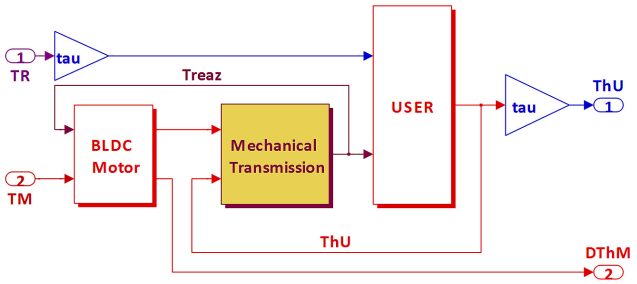

Figure 8. EMA Dynamic Model block diagram.

Figure 8 shows the subsystem simulating the EMA mechanical behavior: it is composed of two non-linear second order dynamic models linked together by means of an instantaneous model simulating the elastic reaction (*Treaz*) dues to shaft stiffness[4]: the first dynamic system is related to the group including motor and gears, while the second one represents the final user. The BLDC Motor and User subsystems implement the second order dynamic models simulating respectively the behaviors of BLDC motor/gear reducer and final user (i.e. the aircraft command surface controlled by the EMA). This type of simulation algorithm, widely explained by Borello, and Dalla Vedova (2012), is also able to simulate the effects of the dry friction forces developed in rotor bearings, gear reducer, hinges and screw actuators; in particular, the frictional torque is calculated by means of the numerical model proposed by Borello, Maggiore, Dalla Vedova and Alimhillaj (2009).

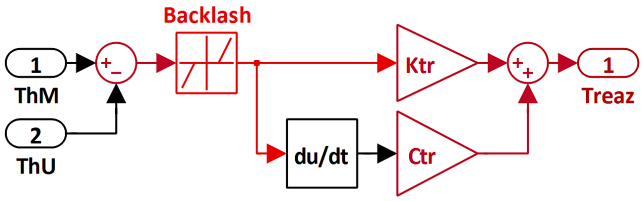

Figure 9. Mechanical Transmission block diagram.

The Mechanical Transmission subsystem shown in figure 9 simulates the behavior of the transmission shaft linking together gear-motor assembly and final user, calculating the corresponding reaction torque (*Treaz*) as a function of *ThM* and *ThU* (respectively motor and user position) and *Ktr* (transmission shaft stiffness) taking into account the effects of the mechanical backlashes.

2 In nominal conditions (no failure considered) the back-EMF acting e.g. on the phase "**a**" is a function of the rotor position *ThM* having the amplitude of *ea* = *ke*·*DThM*, that *ke* is back-EMF constant of the considered phase. In case of electrical failure (such as coil short-circuits or static eccentricity) the back-EMF constants may be suitably modified by means of three functions f(u) (one for each motor phase) properly conceived in order to simulate the effects of these failures.

3 The so obtained mechanical motor torque TM is limited by means of a Simulink Saturation block in order to take in account the actual performance of the real system.

4 It must be noted that the description of the general architecture of the two d.o.f mechanical system employed in the present work and its mathematical model are reported in references [8] and [13].

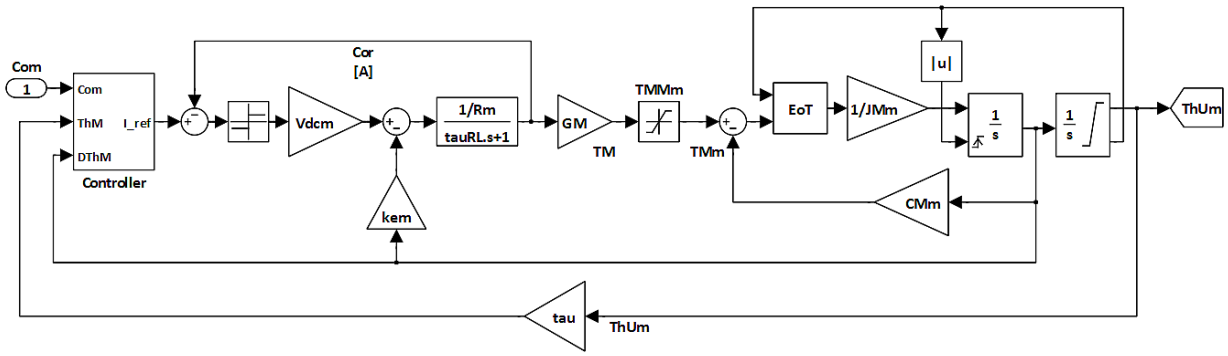

Figure 10. Monitoring Model block diagram.

3. Related Monitoring Model

The above Simulink model, as explained in the previous section, is able to simulate the dynamic behavior of an actual electromechanical servomechanism taking into account the effects due to command inputs, environmental boundary conditions and several failures. So, even with proper limitations, this model allows simulating the dynamic response of the real system in order to evaluate the effects of different faults and designs, analyses and tests different diagnostic and prognostic monitoring strategies. In order to conceive a smart system able to identify and evaluate the progressive failures, it is necessary to compare its dynamic behaviors with the ones provided by an ideal system operating in nominal conditions (in order to neglect the effects due to the aforesaid failures). To this purpose, a new numerical model (more simplified and compact than the previous one), dedicated to monitoring operations, has been developed. As shown in figure 10, the Monitoring Model controller represents a simplified version of the proposed EMA numerical model having the same logical and functional structure; such a model, with respect to the detailed one, is able to give similar performance, although less detailed, requiring less computational effort and reduced computational time.

The Controller calculates the output reference current *I_ref* as a function of the motor angular position *ThM*, the motor angular velocity *DThM* and the commanded position *Com*. In order to simplify the electromagnetic numerical model, the three-phase BLDC motor has been modelled as an equivalent single-phase electromagnetic motor and the driving torque *TM* is directly obtained multiplying the current *Cor* by a torque constant *GM*. The difference between reference (*I_ref*) and actual currents (*Cor*) enters a SIGN block that returns the corresponding phase supply voltage +/-*Vdcm* (respectively, when reference current is higher than actual current or vice versa); these values, decreased of back-EMF, calculates (by means of a transfer function modelling the resistive-inductive circuit) the actual phase current *Cor* used in feedback for motor torque computation *TM*. A saturation block is provided to take into account the corresponding torque limits.

In the aim to simplify the actuator mechanical model, the gearmotor-user assembly has been degraded to a simpler 1 d.o.f. non-linear second order dynamic system (neglecting the effects due to system inertias, transmission shaft stiffness and backlashes and reducing the inertial and viscous terms to the same shaft) and all the friction torques acting on the actual system are ignored.

4. EMA Failures and Degradations

Since EMA have been only recently employed in aeronautics, their cumulated flight hours or on-board installations are not so much to permit to obtain reliable statistics about more recurring failures. However, it is possible to discern between four main categories of failures:

1. mechanical or structural failures;
2. BLDC motor failures;
3. electronics failures;
4. sensor failures.

The present work has been mainly focused on the effects of mechanical failures due to progressive wear, that causes an increase of backlash and friction, and on two typical BLDC motor failures: the coil short-circuits ad the bearing wear generating rotor static eccentricity. Electrical and sensor failures are not less important than the other ones, but their evolutions are usually very fast (if not instantaneous) and the corresponding failure precursors are often difficult to identify and evaluate; nevertheless, it is the intention of the authors to study these types of failure in a next work. As known, dry friction phenomena always occur when two surfaces are in relative motion: when friction coefficients increase due to wear, reaction torque becomes higher and the motor must provide higher torques to actuate the control surface. As shown by Borello, Maggiore, Villero and Dalla Vedova (2010), increased dry friction, while still not causing the seizure of the entire system, reduces the servomechanism accuracy and, sometimes, influences the system dynamic response generating unexpected behavior (stick-slip or limit cycles). The mechanical wear could also generate backlash in EMA moving parts such as gears, hinges, bearings and especially screw actuators.

These backlashes, acting on the elements of the mechanical transmission, reduce the EMA accuracy and can lead to problems of stiffness and controllability of the whole actuator, as shown by Borello and Dalla Vedova (2006). BLDC motor failures are mainly seen as progressive coil short-circuits or bearing wear generating rotor static eccentricity. Short-circuits usually start between a few coils belonging to the same phase (coil-coil failure). Since into short-circuited coils the voltage remains the same and the resistance decreases, a high circulating current arises, generating a localized heating in conductor: this heating favors the extension of the failure to adjacent coils. If this kind of failure is not promptly detected it could propagate and generate phase-phase or phase-neutral damages. The static eccentricity of a rotating body consists in a misalignment between the rotor rotation axis and the stator axis of symmetry; this misalignment is mainly due to tolerances and imperfections during motor construction or to a gradual increase of wear of the rotor shaft bearings. When this failure occurs, the motor having more than one polar couple generates a periodically variable magnetic flux, since the air gap varies during its 360° degrees turn.

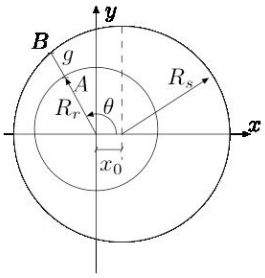

Figure 11. Reference system for the definition of air gap.

In case of static eccentricity, the air gap changes during a spin of the rotor (figure 11) and its behavior can be represented by the function:

$$g'(\vartheta) = g_0 + x_0 \cos(\vartheta) \qquad (1)$$

where g_0, is the clearance between stator and rotor (without considering misalignment) and the second term represents the variation of the air gap with ϑ related to the misalignment x_0; in terms of motor performances, provided torque is lower than in nominal conditions; instead, spectral analysis reveals sub-harmonics increasing for higher eccentricities. The rotor static eccentricity and the partial stator coil short circuit effects have been modeled by means of a simplified numerical algorithm. Since the both failures change the magnetic coupling between stator and rotor, the algorithm simulates the aforesaid failures modifying values and angular modulations of the back-EMF coefficients[5].

5 The proposed algorithm, implemented by means of the functions f(u) contained in the BLDC EM Model block diagram reported in figure 7, acts on the three back-EMF constants *Cei* (one for each branch) modulating their trapezoidal reference values Ke_i as a function of coil short circuit percentage, static rotor eccentricity ζ and angular position ϑ_r.

$$ke\_a = Ke_i \cdot Ce_i \cdot (1 + \zeta \cdot \cos(\vartheta_r)) \qquad (2)$$

The so obtained constants (*ke_a*, *ke_b*, *ke_c*) are then used to calculate the corresponding counter-electromotive forces (*ea*, *eb*, *ec*) and to evaluate the mechanical couples (*Cea*, *Ceb*, *Cec*) generated by the three motor phases (figure 7).

5. FAULT DETECTION/EVALUATION ALGORITHMS

As already said, prognostics is an engineering discipline whose purpose is to predict an incipient failure of a certain component, allowing possible interventions before the initial flaw propagates. The failure detection/evaluation could be achieved by means of a proper algorithm (typically applied to a numerical model) able to detect the failures and predict their evolution. This fact underlines a limit of prognostics: it could predict only failures which presents a gradual growth and it is not able to detect sudden faults. Prognostics algorithms can have several complexity levels, from the simplest based on heuristic criteria to the most complex involving physical failure models. Developing a prognostic algorithm able to identify the precursors of an EMA failure and its degradation pattern is thus beneficial for anticipating the incoming failure and alerting the maintenance crew such to properly schedule the EMA replacement. This avoids a servomechanism failure in service, thereby ensuring improved equipment availability and minimizing the impacts onto the logistic line. To this effect, a model based failure detection/evaluation technique was developed that fuses several information obtained by comparing actual with expected responses of the EMA to recognize a degradation and estimate the remaining useful life. The choice of the best algorithms able to detect and evaluate a particular kind of incipient failure is driven by their ability to detect the failure itself, so proper tests are needed. The proposed algorithm is based upon:

1. Fourier spectral analysis (by means of FFT);
2. Correlation coefficient.

The Fourier Transform (FT) is a mathematical instrument, based upon the theory of Fourier series, which has many applications in physics and engineering (Welch 1967). Fourier Transform of a function *f(t)* is often calculated by means of the Discrete Fourier Transform (called DFT). Unlike the typical FT, the DFT requires as input a discrete function; this restrains the DFT to the analysis of a function on a limited and discrete domain. It must be noted that the input values of DFT are finite sequences of real or complex numbers, feature that makes it ideal for data processing on electronic calculators; in particular, this method is employed to analyze the frequencies composing a certain numerical signal by means of proper algorithms constituting the Fast Fourier Transform (FFT) (as shown by Cardona, Lerusse and Géradin 1998). In order to achieve the spectral analysis of the dynamic response of the actuation system to a given command, a dedicated numerical algorithm (based upon the FFT MATLAB implementation) has been conceived.

As mentioned earlier, the other instrument used to detect incipient failures or wear conditions is the correlation coefficient C. This coefficient, as proposed by Borello, Dalla Vedova, Jacazio and Sorli (2009) and Dalla Vedova et al. (2010), is defined as:

$$C = \frac{\int_0^T x_T x_M dt}{\int_0^T x_T^2 dt} \quad (3)$$

where x_T is the set of observed data and x_M is the theoretical data: in this work, they are respectively the results of the model that simulates the actual system and the data from the monitoring model. The data considered in the two vectors, depending on the case, could concern positions, velocities or other physical magnitudes of the system. The data representing the dynamic response of the actual system (fault sensitive) are compared with the results provided by the monitoring system (that simulates ideal conditions, since no progressive failures are considered): the more the failure is considerable, the more the results obtained from the simulated actual system differ from the theoretical data[6]. This difference, in order to be useful for prognostic analysis, should have a monotonic trend related to the corresponding failure increase. In order to allow a direct correlation between the growth of a defined failure and the corresponding value of the correlation coefficient, it is necessary to identify a physical magnitude (sensitive to the aforesaid failure) that, with increasing failure itself, generates a monotonic and easily detectable trend of C; to this purpose, the authors have conceived another dedicated numerical algorithm (developed in MATLAB environment) implementing equation (3).

6. FAILURES EFFECTS OF THE EMA BEHAVIOR

In order to recognize the effects produced by a failure on the dynamic behavior of the considered actuation system, the dynamic responses generated under such conditions are compared with those reported in nominal conditions (i.e. considering the nominal values of parameters and failures). The proposed EMA model has been tested with several simulations in nominal conditions (NC): the compliance between the actual behaviors of a real EMA and the corresponding simulated results have been evaluated by means of many types of *Com*; subsequently, these results have been compared with the system behavior in failure conditions. A step command input (figure 12) generates a dynamical response that, in NC (having proper values of dry friction torque and mechanical backlash and neglecting any phase short circuit or rotor static eccentricity), puts in evidence the system stability margin, the non-linear effects due to saturations and the position errors due to frictions (this is because the authors model integrates the dry friction algorithm in a dynamic system able to take into account also the hard stops effects and their mutual interactions); by this way it is possible to discern between static and dynamic friction conditions and evaluate their effects on the system. Figure 13 puts in evidence the EMA numerical model ability to simulate the actual dynamics of the three-phase currents (*Ia, Ib, Ic*) taking into account the effects due to PWM regulation ad phase commutation, such as "two-phase on" effect shown by Haskew, Schinstock and Waldrep (1999) or Hemanand and Rajesh (2006).

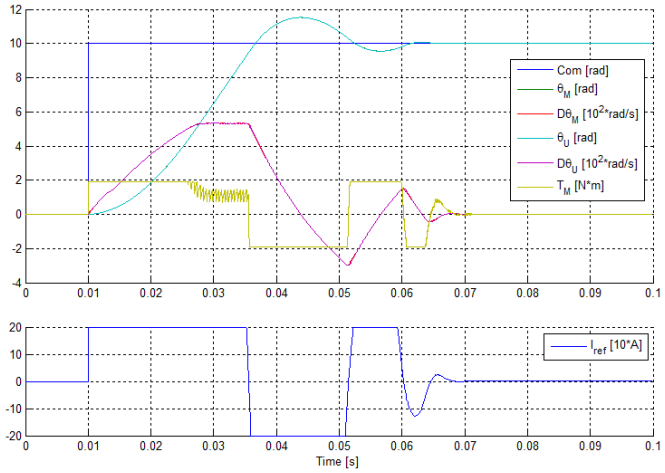

Figure 12. Example of system dynamic behavior in condition of step position command.

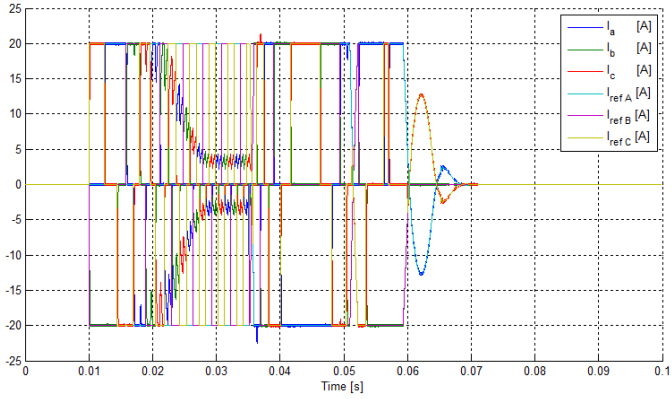

Figure 13. Related reference and actual phase.

The ramp response analysis reveals that the proposed model is able to simulate both a high-slope ramp response (Fig. 14) and a stick-slip phenomenon (Fig. 15); the first case underlines the limits of the actuator in terms of maximum speed, while the latter shows what occurs when the ramp slope is lower enough to emphasize the frictional effects. Furthermore, the model allows to evaluate the incipient motion resolution of the servomechanism, i.e. the smallest command value producing an actuator's response. Obviously, this value becomes higher as frictional contribution is more significant, that is when the servomechanism undergoes increasing wear conditions.

6 If the vector of observed data exactly corresponds to the theoretical data, C is equal to 1. If this correspondence does not occur, the more the discrepancy between the two data sets is noticeable, and the more the value of C is different from 1: its value could be higher or lower than 1.

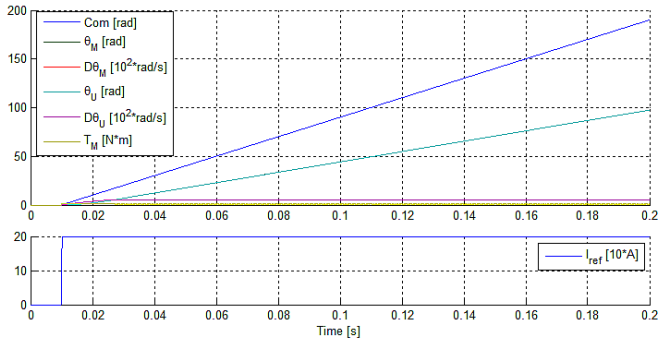

Figure 14. Example of system dynamic behavior in condition of high slope ramp command.

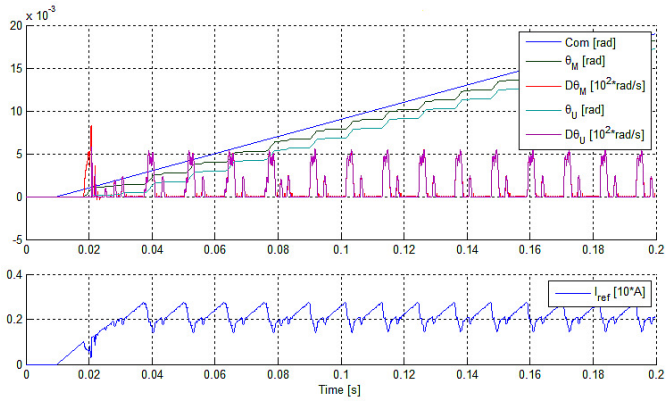

Figure 15. Example of system dynamic behavior in condition of very low slope ramp command.

At the same way, several periodic inputs have been examined confirming the model ability to simulate the behavior of the real actuation system and its sensitivity to nonlinear effects, command inputs (in terms dynamic response related to amplitude and frequency input) and external loads. The most interesting results are provided by FFT analysis performed on positions and velocities of motor and user. The algorithm employed to perform this task correctly records the most important spectral contribution of the analyzed magnitudes as a function of the corresponding command frequency: its amplitude is related to the command semi-amplitude. If the given command has an amplitude or a frequency too wide to be properly followed by the servomechanism, this analysis also records odd multiple harmonics of the command frequency (which typically appear if signals distortions have a half-wave symmetry). Checked the compliance of the proposed numerical model in NC, several analysis have been performed considering the four possible failures.

Firstly, the effects of wear conditions (friction and backlash) have been evaluated: the friction torque is defined as a percentage of the maximum motor torque, while the mechanical transmission backlash is modeled as localized downstream the gear reducer.

The high-slope ramp command provides significant results:

1. In terms of FFT analysis on velocities, the fundamental frequency recorded in nominal conditions is around 2040 Hz. This value slightly decreases as frictional effects increase, since angular velocity is reduced by friction. The amplitude related to this frequency monotonically increases with friction and increasing non-monotonic multiple harmonics arise (the second and the third ones have been recorded during FFT analysis). Backlash is not detected with FFT algorithm;
2. The investigation on the correlation coefficients reveals that on user position and velocity a negligible increase with friction has been found, while a definite decreasing monotonic trend can be recorded for motor torque. The same analysis performed on backlash has not provided any employable data, from a prognostic point of view. The correlation coefficient for reference current is always 1 for a ramp input, since the actuator follows a velocity regime and this fact is independent from the kind of failure implemented on the model.

Further analysis concern the sinusoidal response (the input has a frequency of 20 Hz and an amplitude of 0.001 rad):

1. FFT analysis cannot detect nor friction nor backlash, since only the command frequency prevails;
2. All the correlation coefficients generally show negligible variations (lower than 1%), regardless of changes in command frequency or amplitude. The exceptions are motor torque and reference current, which show similar monotonic, decreasing trends as friction grows: this behavior is due to the higher torque needed to follow the command. This trend, clearer for friction and less remarked for backlash, is similar for both the wear effects.

Secondly, the effects of electrical failures on the performances of the servomechanism have been evaluated, considering coil short-circuit and rotor static eccentricity. A typical behavior of the system undergoing electrical failures is the rise of sub-harmonics on the spectra of angular velocities. This phenomenon is clearly recorded with the FFT analysis on the high-slope ramp command:

1. 1/3 and 2/3 multiple of the fundamental harmonic are related to short-circuits; the 1/3 harmonic provides the most important contribution in terms of amplitude when the failure ratio is above 0.02;
2. 1/6 and 1/2 multiple harmonics concern the rotor static eccentricity. In this case, the 1/6 harmonic is the prevailing term for misalignments higher than 1%.

These sub-harmonic values could be explained by means of this relation:

$$\frac{f_M}{f_{\omega,M}} \cong 2 * p * n \qquad (4)$$

where f_M is the fundamental frequency recorded by FFT motor velocity analysis, $f_{\omega,M}$ is the motor velocity in Hz, $p=4$ is the number of polar couples, $n=3$ is the number of phases. For sub-harmonics induced by coil failures, it is clear that they arise due to differences in the n motor phases, so the spectral analysis detects significant contributions at $\frac{i}{n} \cdot f_M,\ i = 1,..,n$. The rotor static eccentricity, instead, is represented on the spectrum as combined by a sub-harmonic related to the number of polar couples p (i.e. the 1/6 sub-harmonic, for this motor) and the 1/2 sub-harmonic. The latter represents the effect of the eccentricity on a certain polar couple. In both cases the sub-harmonic amplitudes show a monotonic trend: this result allows to detect a possible electrical failure with a simple observation of FFT spectra. In this case, only the correlation coefficient for motor torque shows monotonic trends for both the failures. The sinusoidal command provides the following results:

1. As for wear detection, the FFT analysis fails due to the predominance of the command frequency;
2. Significant results are provided by the analysis on correlation coefficients: in particular, a significant decreasing monotonic trend can be recognized in reference current for coil failures.

Finally, the open-loop step response has been evaluated: all the analyzed magnitudes show monotonic trends in terms of correlation coefficients for both failures, but the variations are not significant enough to be employed in prognostics.

7. FAILURE MAPS

After the analysis performed on a single acting failure, this work focuses on the effects due to the simultaneous presence of different kinds of failures acting on the system. To the purpose to achieve a timely identification and evaluation of these failures, the authors developed a new faults detection technique based on failure maps (FMs). A failure map constitutes the graphical representation of how a system-representative parameter varies as a function of two different types of failures; in other words, if the measurement of the parameter of the real system is available, this instrument allows to suppose which extent a certain couple of failures has on the actuator. More exactly, a failure map displays the first failure G_1 on x-axis and the representative parameter P_1 on y-axis. Each map represents a set of curves $P_1 = f(G_1)$ which are parameterized with the second failure G_2. A proper choice of P_1 is crucial in order to obtain a useful failure map. Firstly, this parameter should be a function of both $G_1$and G_2. It is preferable a parameter which is highly sensitive to changes in failure levels. In particular, its dependence from the two kinds of failure should be monotonic, i.e. the curves plotted on the maps should not intersect: this feature is the most important, since it allows to detect a specific area on the map containing all the possible failure levels.

The proposed prognostic technique, in order to identify system conditions with high enough accuracy, requires more than one of these maps for a specific couple of failures. When several maps are employed, it is important that they are independent from each other. Independent maps can be obtained when the actuator undergoes different command inputs: in this way, the parameter represented on each map is a magnitude that is not related to the others. By using three independent maps, i.e. representing three different parameters P_1, P_2 and P_3, an accurate area containing the possible failures is identified. The considered inputs are:

1. A sinusoidal input with a frequency of 20 Hz and an amplitude of 0.001 rad;
2. A high-slope ramp command at 10 rad/s;
3. A step command with an amplitude of 0.005 rad, with the actuator in open-loop configuration.

By using the results found during the single failure analysis to find the most suitable parameter for the map drawing, all the possible failure combinations have been investigated. It must be noted that, in many cases, the FMs were not suitable for prognostics; for few couples there were not enough independent maps (as for the couple *coil failure – rotor static eccentricity*, with only two employable maps). A couple on which the method has been successfully tested was the *friction – coil failure* couple, allowing to obtain more independent maps. Among these, three were chosen to apply the FMs method (G_1= friction, G_2i= coil failure ratio).

The first map (figure 16) concerns correlation coefficient C for reference current, P_1, obtained with sinusoidal input.

The second map (figure 17) represents the correlation coefficient C for user position, P_2, when a step input is given to the open-loop system (OL).

Finally, the last map (figure 18) shows the response to a high-slope ramp input in terms of the correlation coefficient C for user velocity, P_3.

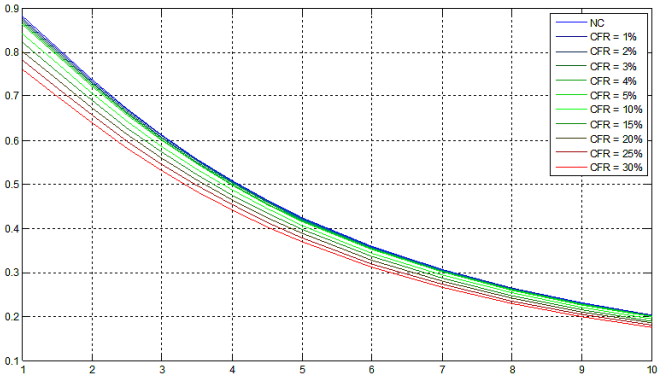

Figure 16. Correlation coefficient C failure map related to reference current – Sinusoidal input.

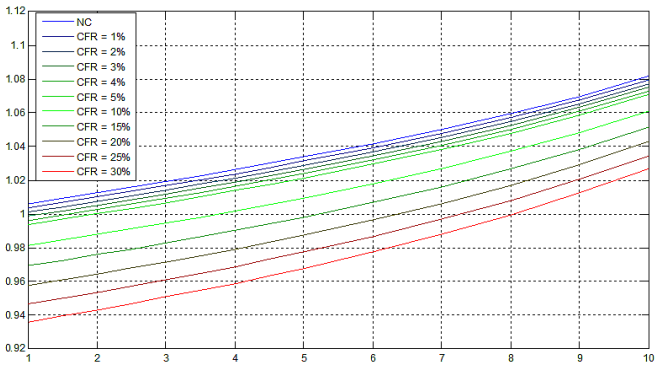

Figure 17. Correlation coefficient C failure map related to user position – OL Step input.

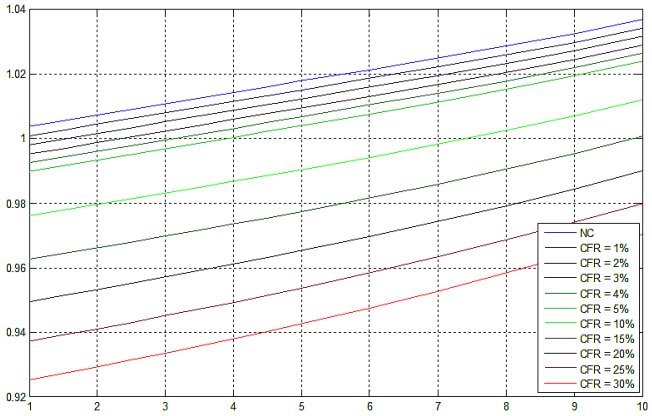

Figure 18. Correlation coefficient C failure map related to user velocity – High slope ramp input

After the maps have been obtained, they can be employed for the proposed procedure, which is now explained in detail. Firstly, the numerical model is simulated as affected by a known level of both friction and coil failure ratio, considering the three different command inputs: this step provides the parameters P_1, P_2 and P_3. As these values will employed on the failure maps, a certain statistical dispersion, equal to a ±5% of the maximum variation between the curves of each map is taken into account. Then, the first map is employed with the entering value of P_1 and an initial large area containing the possible failure levels for G_1 and G_2 is obtained. These two intervals are inserted on the second map, which requires also the value P_2: their intersection provides narrower intervals of the two kinds of failure. The procedure applied on the third map (on which P_3 is considered) is the same seen for the second one. This method have been successfully employed on a number of combinations of friction and coil failure ratio, always resulting on an enough accurate detection of the failure levels acting on the actuator.

The example shown in figure 19 is referring to a friction torque equal to four times the nominal value (4·NC), a 4% of the coil failure ratio and a rotor static eccentricity ratio equal to 0.05: the *X* represented the supposed failure level.

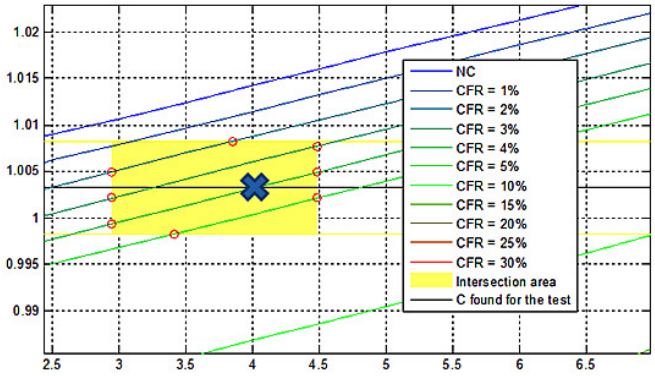

Figure 19. Example of application of Failure Maps

It must be noted that the correlation coefficients considered are not significantly sensitive to the variations induced in the system by low levels of backlash or rotor static eccentricity; so, the levels of friction and coil short-circuit could be properly recognized neglecting their effects.

8. CONCLUSIONS

This work focuses on the research of system-representative parameters which are suitable for prognostic activities and on the development of a technique, allowing a prompt detection of gradually-increasing failures on aircraft actuators. The study has been performed on a numeric test bench (simulating the behavior of a real EMA actuator) that implements four kinds of failure: friction, backlash, coil short circuit, rotor static eccentricity; by means of proper simplifications, the aforesaid numerical model was then reduced obtaining the monitoring model. The proposed failure detection/evaluation algorithm has been developed mixing together the information derived from the spectral analysis of signals (performed by means of the FFT algorithm) and by direct comparison between EMA and monitoring model (through the correlation coefficient C); by means of these tools suitable fault precursors, useful for early recognition and quantification of the damage, have been identified. Finally, proper failure maps have been drawn to perform the analysis of combined failures. This method have been successfully applied to many different combinations of considered failures, guaranteeing always an enough accurate detection/estimation of their levels.

REFERENCES

Çunkas, M., & Aydoğdu, O. (2010). Realization of Fuzzy Logic Controlled Brushless DC Motor Drives using Matlab/Simulink. *Mathematical and Computational Applications*, vol. 15, n. 02, pp. 218-229.

Halvaei Niasar, A., Moghbelli, H., & Vahedi, A. (2009). Modelling, Simulation and Implementation of Four-Switch Brushless DC Motor Drive Based On Switching Functions. *IEEE EUROCON 2009*. May 18-23, St.-Petersburg (Russia), pp. 682 – 687.

Borello, L., Maggiore, P., Dalla Vedova, M. D. L., Alimhillaj, P. (2009). Dry Fiction acting on Hydraulic Motors and Control Valves: Dynamic Behavior of Flight Controls. *XX National Congress AIDAA*. Milan (Italy)

Borello, L., Maggiore, P., Villero, G., & Dalla Vedova, M. D. L. (2010). A comparison between Dry Friction Discontinuous Computational Algorithms. *27th International Congress of the Aeronautical Sciences ICAS 2010*. September 19-24, Nice (France).

Borello, L., & Dalla Vedova, M. D. L. (2012). A Dry Friction Model and Robust Computational Algorithm for Reversible or Irreversible Motion Transmission. *International Journal of Mechanics and Control (JoMaC)*, vol. 13, n. 02, pp. 37-48, ISSN: 1590-8844.

Borello, L., Dalla Vedova, M. D. L., Jacazio, G., & Sorli, M. (2009). A Prognostic Model for Electrohydraulic Servovalves. *Proceedings of the Annual Conference of the Prognostics and Health Management Society*. September 27-October 1, San Diego (USA).

Dalla Vedova, M. D. L., Jacazio, G., Maggiore, P., & Sorli, M. (2010). Identification of Precursors of Servovalves Failures for Implementation of an Effective Prognostics. *International Conference of Recent Advances in Aerospace Actuation Systems and Components*. May 5-7, Toulouse (France), pp.116-126.

Borello, L., & Dalla Vedova, M. D. L. (2006). Mechanical failures of flap control systems and related position errors: proposal of innovative configuration equipped with centrifugal brakes. *International Journal of Mechanics and Control (JoMaC)*, vol. 07, n. 02, pp. 7-20, ISSN: 1590-8844.

Welch, P. D. (1967). The Use of Fast Fourier Transform for the Estimation of Power Spectra: A Method Based on Time Averaging Over Short, Modified Periodograms. *IEEE Transactions on audio and electroacoustics*, vol. AU-15, n. 2.

Cardona, A., Lerusse, A., & Géradin, M. (1998). Fast Fourier nonlinear vibration analysis. *Computational Mechanics*, vol. 22, n. 02, pp. 128-142.

Lee, B. K., Ehsani, M. (2003). Advanced Simulation Model for Brushless DC Motor Drives. *Electric Power Components and Systems*, vol. 31, n. 9, pp. 841–868, ISSN: 1532-5008.

Hemanand, T., Rajesh, T. (2006). Speed Control of Brushless DC Motor Drive Employing Hard Chopping PWM Technique Using DSP. *Proceedings of India International Conference on Power Electronics (IICPE 2006)*. December 19-21, Chennai (India), pp. 393-396.

Haskew,T. A., Schinstock, D. E., & Waldrep E. M. (1999). "Two-Phase On" Drive Operation in a Permanent Magnet Synchronous Machine Electromechanical Actuator. *IEEE Transactions on on Energy Conversion,* vol. 14, v. 02.

BIOGRAPHIES

Paolo Maggiore is a professor at the Mechanical and Aerospace Engineering Department of Politecnico di Torino, that joined in 1992, where he teaches aerospace general systems engineering. Currently his students are involved in projects ranging from hydrogen fuel cell powered airplanes and UAVs, and health monitoring of flight controls, to multi-disciplinary design optimization of aerospace systems design.

Matteo D. L. Dalla Vedova received the M.Sc. and the Ph.D. from the Politecnico di Torino in 2003 and 2007, respectively. He is currently assistant researcher at the Department of Mechanics and Aerospace Engineering. His research activity is mainly focused on the aeronautical systems engineering and, in particular, is dedicated to design, analysis and numerical simulation of on board systems and developing of prognostic algorithms for flight control systems and aerospace servomechanism.

Lorenzo Pace graduated in Aerospace Engineering at Politecnico di Torino in 2008. Since 2008 to 2011, he worked as an assistant researcher, following studies about system experimental testing and modelization in the aerospace field, with a focus to energy saving techniques. Since 2012 he is completing a PhD in Aerospace Engineering at Politecnico di Torino, with the contribution of Thales Alenia Space, focused on the application of Model Based System Engineering to verification in the space industry.

Alessio Desando graduated in Aerospace Engineering at Politecnico di Torino in 2013. His Master Degree thesis is focused on prognostic techniques for actuators. He is currently working as a research assistant from May 2013, performing studies on labyrinth seals and cyclonic separators.